第 48 卷 第 20 期/2021 年 10 月/中国激光 研究论文

中国激光

Nd:YVO_4激光器横模频率简并现象的研究

林达[1,2]，王晶[1,2]，李丙轩[1]，廖文斌[1]，林长浪[1]，汤凯飞[1,3]，李柯[1,2]，张戈[1*]

[1]中国科学院福建物质结构研究所光电材料化学与物理重点实验室，福建 福州 350002；

[2]中国科学院大学，北京 100049；

[3]福州大学化学学院，福建 福州 350108

摘要 精确的简并范围是运用横模频率简并原理产生结构光场的重要条件。本文基于激光频谱研究了共焦腔处于 1/2 简并态时激光横模频率简并的现象，并提出一种更准确的简并范围测量方法。实验中详细观测输出激光频谱信号随腔长的变化。利用频谱信息，实现了对腔内不同阶横模在发生简并时动力学行为变化的监测。研究结果表明，当腔内不同阶横模发生频率简并时，不同简并族的横模未因模式竞争被抑制，而是共存于腔内。同时，利用激光频谱随腔长的变化，实现了对简并范围更准确的测量。简并过程中重点监测的两个频率信号随着腔进入简并态合并成一个频率信号，该状态在一段腔长范围内稳定存在。据此测得更精确的简并范围，对应腔长约为 0.20 mm。此外，对实验中测得的频谱信号进行理论对比，频谱信号的实验值与理论值基本吻合。

关键词 激光器；横模；频谱；简并；简并范围

中图分类号 O432.1+2 **文献标志码** A **doi**：10.3788/CJL202148.2001003

1 引 言

近年来，结构光越来越多地被应用于各个领域，例如光镊[1]、螺旋干涉仪[2]和相位差显微镜[3]等。获得结构光的途径通常是利用空间光调制器或螺旋相位片等器件。但这种在激光腔外对光束进行整形的方法存在功率上的限制，而且对器件结构的要求较高，所以其应用有一定的局限性。为使激光器直接输出结构光，可在腔内利用横模频率简并[4]（或横模锁定）原理，使输出激光呈现某些特殊的结构性光斑。精确的简并范围是运用横模简并原理的重要前提，一般只有在简并范围内，腔内的不同横模才可能发生频率简并，进而相干叠加形成稳定的结构性光场。

许多研究人员对激光横模及其频率简并现象展开了广泛的探索[5-15]。Bezotosnyi 等[11]指出，由于增益介质具有色散和增益非均匀性，每个腔的简并态都存在两个简并长度。在这两个简并长度范围内，腔基模都不同于高斯模，并且这两个长度内的腔基模的光强分布方向相互垂直；Bezotosnyi 等[12]还从理论和实验上研究了腔长处于简并范围时激光器阈值泵浦功率的变化。经研究发现，当腔处于临界简并态时，激光器阈值泵浦功率明显下降。这些研究都侧重于展示和分析横模频率简并的结果，对于简并过程的研究相对较少，并且提及的简并范围精度仍可进一步提高。

为研究横模频率简并过程及得到更精确的简并范围，本文利用输出激光的频谱，通过观测其变化来表征横模频率简并的过程。由此分析简并过程中不同阶横模的动力学行为，并得到更精确的简并范围。

2 基本原理

在激光腔内，横模发生简并的重要条件是谐振腔处于简并态，即该腔是简并腔[16]。Francia[17]曾指出，如果一个谐振腔满足腔内任一光束在一次或多次往返后都能重复其轨迹，那么这个谐振腔亦可

收稿日期：2021-02-24；**修回日期**：2021-03-19；**录用日期**：2021-03-29

基金项目：国家自然科学基金（61875199，61975208，51761135115）、中国科学院战略重点研究计划（XDB20000000）、福建省科学基金（2019J02015）

通信作者：*zhg@fjirsm.ac.cn

认为是简并腔。

给定一个谐振腔，腔长为 L，则腔的模式频率可表示为

$$w_{q,n,m}=\left[q+(n+m+1)\cdot\frac{\arccos(\pm\sqrt{g_1\cdot g_2})}{\pi}\right]\cdot\frac{\pi\cdot c}{L},\tag{1}$$

式中：q 表示纵模参数；m 和 n 表示横模参数；$g_{1,2}=1-L/R_{1,2}$，为谐振腔的参数，其中 $R_{1,2}$ 为腔镜的曲率半径。

如果两个模式发生频率简并，也就是它们的频率相等，即

$$w_{q,n,m}=w_{q+\Delta q,n+\Delta n,m+\Delta m},\tag{2}$$

结合(1)式和(2)式，可得：

$$\frac{-\Delta q}{\Delta m+\Delta n}=\frac{\arccos(\sqrt{g_1\cdot g_2})}{\pi}。\tag{3}$$

令 Δf_{T} 表示横模间距，Δf_{L} 表示纵模间距，那么(3)式可表示为

$$\frac{\Delta f_{\mathrm{T}}}{\Delta f_{\mathrm{L}}}=\frac{\arccos(\sqrt{g_1\cdot g_2})}{\pi}=\frac{\arccos\left[\sqrt{(1-L/R_1)\cdot(1-L/R_2)}\right]}{\pi}。\tag{4}$$

若一谐振腔满足 $\Delta f_{\mathrm{T}}/\Delta f_{\mathrm{L}}=r/s$（$r/s$ 是不可约分数）[12]，则该谐振腔即处于 r/s 简并态。本实验中，当腔长 L 为 50.00 mm 时，结合腔镜曲率半径 $R_1=R_2=50$ mm，代入(4)式可得：$r/s=\Delta f_{\mathrm{T}}/\Delta f_{\mathrm{L}}=1/2$，即谐振腔处于 1/2 简并态。在 1/2 简并态，腔内横模根据频率简并理论分成两族，一族包含 TEM_{00}、TEM_{02} 和 TEM_{04} 等模式，另一族包含 TEM_{01}、TEM_{03} 和 TEM_{05} 等模式。这两族模式之间存在一频差，即横模间距 Δf_{T}。为了更直接地研究横模频率简并的过程，本实验重点关注输出激光频谱随腔长的变化情况。

3　实验与分析

本实验将光纤耦合的半导体激光器作为泵浦光源，光纤直径为 200 μm。谐振腔型为共焦腔，输入镜(IM)和输出镜(OC)皆是曲率半径为 50 mm 的平凹镜。输入镜对波长为 808 nm 的光的反射率为 8.68%，对波长为 1064 nm 的光的反射率为 99.98%。输出镜对波长为 1064 nm 的光的反射率为 98.18%。实验中使用的激光晶体是 a 切向的浓度(原子数分数)为 1.0% 的 $\mathrm{Nd:YVO_4}$，尺寸为 5 mm×5 mm×0.3 mm。因晶体较薄，冷却方式采用空冷。晶体处泵浦光斑的直径约为 290 μm，泵浦功率约为 0.9 W。将输出镜固定在一平移台上，可持续调整腔长。实验中腔长在 45.25～55.25 mm 范围内变化，在简并位置附近，腔镜的移动步长为 0.05 mm。输出激光经一焦距为 150 mm 的透镜聚焦后入射到探测器(Thorlabs Inc. DET08CL/M)中，探测器与频谱仪(Radio Frequency Signal Analyzer，Keysight N9000A CXA)连接(图 1)。

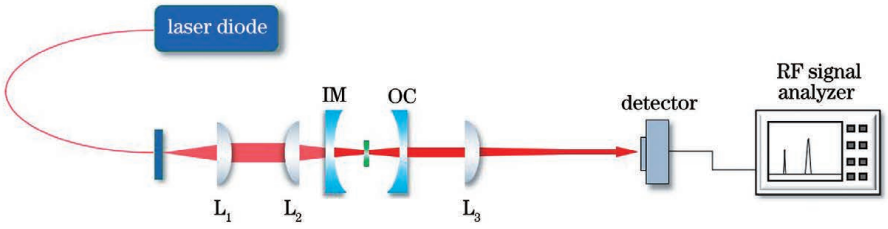

图 1　实验装置示意图

Fig. 1　Schematic of experimental setup

图 2 为实验中改变腔长时，在一个纵模间距内(即 0～3 GHz 范围内)检测到的输出激光频率信号及其理论值的对比图。整体上，各频率信号的实验值与理论值基本吻合。随着腔长改变，不同阶横模之间的拍频信号发生规律性变化。根据此规律，可以通过激光频率的变化监测不同阶横模在简并过程中的行为变化。Δf_{T} 和 $\Delta f_{\mathrm{L}}-\Delta f_{\mathrm{T}}$ 为相邻阶横模的拍频，如图 3 所示，$\nu_2-\nu_1=\Delta f_{\mathrm{T}}$，$\nu_3-\nu_2=\Delta f_{\mathrm{L}}-\Delta f_{\mathrm{T}}$，$\Delta f_{\mathrm{T}}$ 可理解为 ν_1 和 ν_2 之间的拍频，$\Delta f_{\mathrm{L}}-\Delta f_{\mathrm{T}}$ 为 ν_2 和 ν_3 之间的拍频。Δf_{T} 和 $\Delta f_{\mathrm{L}}-\Delta f_{\mathrm{T}}$ 的存在说明腔内相邻横模在谐振腔处于简并态时，虽然不属于同一简并族，但其中一族未因为模式竞争被抑制，它们一直在腔内共存。$\Delta f_{\mathrm{L}}-2\Delta f_{\mathrm{T}}$ 和 $2\Delta f_{\mathrm{T}}$ 是非相邻阶但属于同一简并族(发生简并时)的横模之间的拍频。在图 3 中，$\Delta f_{\mathrm{L}}-2\Delta f_{\mathrm{T}}$ 和 $2\Delta f_{\mathrm{T}}$ 可理解为 0 阶和 2 阶横模之间的拍频，$\Delta f_{\mathrm{L}}-2\Delta f_{\mathrm{T}}=\nu_3-\nu_4$，$2\Delta f_{\mathrm{T}}=\nu_4-\nu_1$。当共焦腔远离 1/2 简并位置时，$\Delta f_{\mathrm{L}}-2\Delta f_{\mathrm{T}}\neq 0$，$2\Delta f_{\mathrm{T}}\neq\Delta f_{\mathrm{L}}$，非相邻阶但属于同一简并族的横模未进入简并状态。随着共焦腔接近简并位置，$\Delta f_{\mathrm{L}}-2\Delta f_{\mathrm{T}}$ 趋向于 0，而

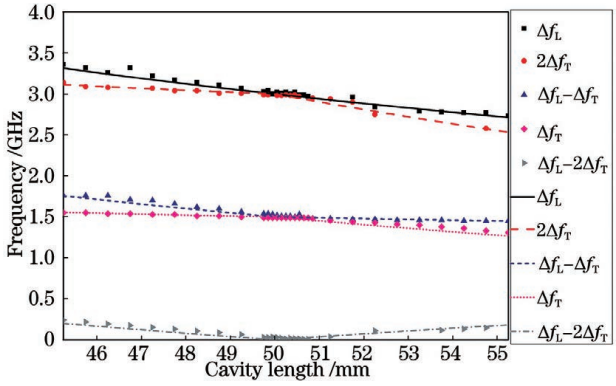

图 2　实验中测到的频谱信号及其理论计算值，其中线条表示理论值，散点表示实验值

Fig. 2　Laser frequency signals measured in the experiment and their theoretical values. Line indicates theoretical value and scatter indicates experimental value

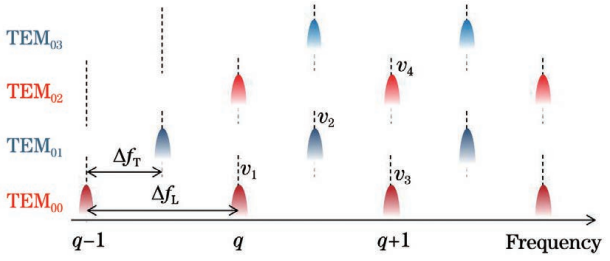

图 3　1/2 简并态的频率简并示意图

Fig. 3　Schematic of frequency degeneracy in 1/2 degenerate state

$2\Delta f_T$ 逐渐与 Δf_L 在数值上趋于一致。此时 0 阶和 2 阶横模发生频率简并，理论上无法在频率上区分二者。但是，除基横模外的每一阶横模都不只包含一个横模成分，比如 2 阶横模中包含 TEM_{02}、TEM_{20} 和 TEM_{11} 模式，模式之间存在一定的频差，因此在简并位置 $\Delta f_L-2\Delta f_T$ 不等于 0，而是等于一个很小的值，如图 2 所示。理论上，$2\Delta f_T$ 频率信号在简并位置应该消失，但由于腔内是多纵模运行状态，在简并位置 $2\Delta f_T$ 等于纵模间距，因此该频率成分仍存在。

图 2 反映了不同阶横模在发生频率简并时的动力学行为变化。相邻阶横模在腔进入简并态时并未因模式竞争被抑制；非相邻阶但属同一简并族（简并发生时）的横模在简并位置发生简并，谐振输出。在简并位置可比较明显地观测到同一阶横模（除基横模外）内部的不同横模成分之间的频差，但在非简并位置未明显检测到相应的频差。

不同腔长时光斑强度分布如图 4 所示。因为泵浦光聚焦后晶体处光强呈现外圈强、中心弱的状态，输出激光的光强分布近似环形；并且由于谐振腔存在像散，光斑呈现出一定的椭圆度。从图 4 可以看出，随着谐振腔进入简并态，腔内激发出更多的横模。这可能是因为高阶横模与低阶横模发生频率简并后，其泵浦阈值降低[12]，最终与低阶模谐振输出。

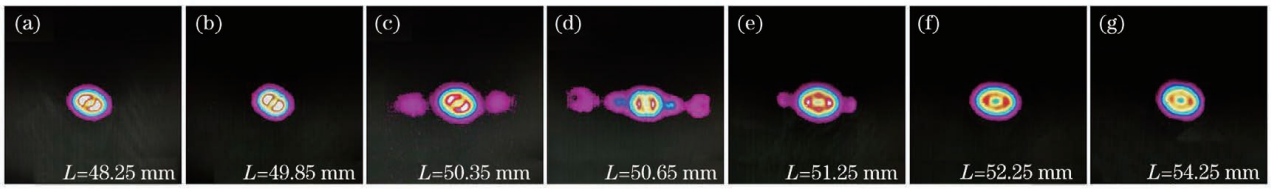

图 4　不同腔长时的光斑强度分布

Fig. 4　Beam intensity distribution at different cavity lengths

图 5 为不同腔长时输出激光的频谱图，该频谱图是在 1.5 GHz 附近测得。图 5 所示的两个拍频信号即图 2 中的 Δf_T 和 $\Delta f_L-\Delta f_T$。在 1/2 简并位置，Δf_T 的理论值为 1.5 GHz，Δf_L 的理论值为 3.0 GHz，$\Delta f_T=\Delta f_L-\Delta f_T$。因此，随着共焦腔逐渐接近 1/2 简并位置，这两个拍频信号在频谱上逐渐靠近，最终合并成一个频率信号，即这两个频率成分发生简并。图 5 清楚地呈现出此简并过程，并且在一个较小的腔长范围内，频率简并的状态可稳定存在，如图 5(e)、(f)所示。利用此频谱信号变化，实现了对简并范围（本文把频率发生简并的范围称作“简并范围”）更准确的测量。本实验中，简并范围对应的腔长约为 0.20 mm。在一些文献中，简并范围（或锁定范围）主要是由阈值泵浦功率的变化[12]或输出功率曲线的变化[18]来确定，由此确定的简并范围相对宽泛，其精度可进一步提高。本实验利用激光频谱确定的简并范围精度更高，相对更准确。

4　结　　论

从频谱的角度观测及分析激光横模频率简并的过程。实验上，通过观测腔长持续变化时的激光频谱信号，实现对不同阶横模动力学行为变化的监测。属于不同简并族的横模在谐振腔处于简并态时未因模式竞争被抑制，而是共存于腔内；属于同一简并

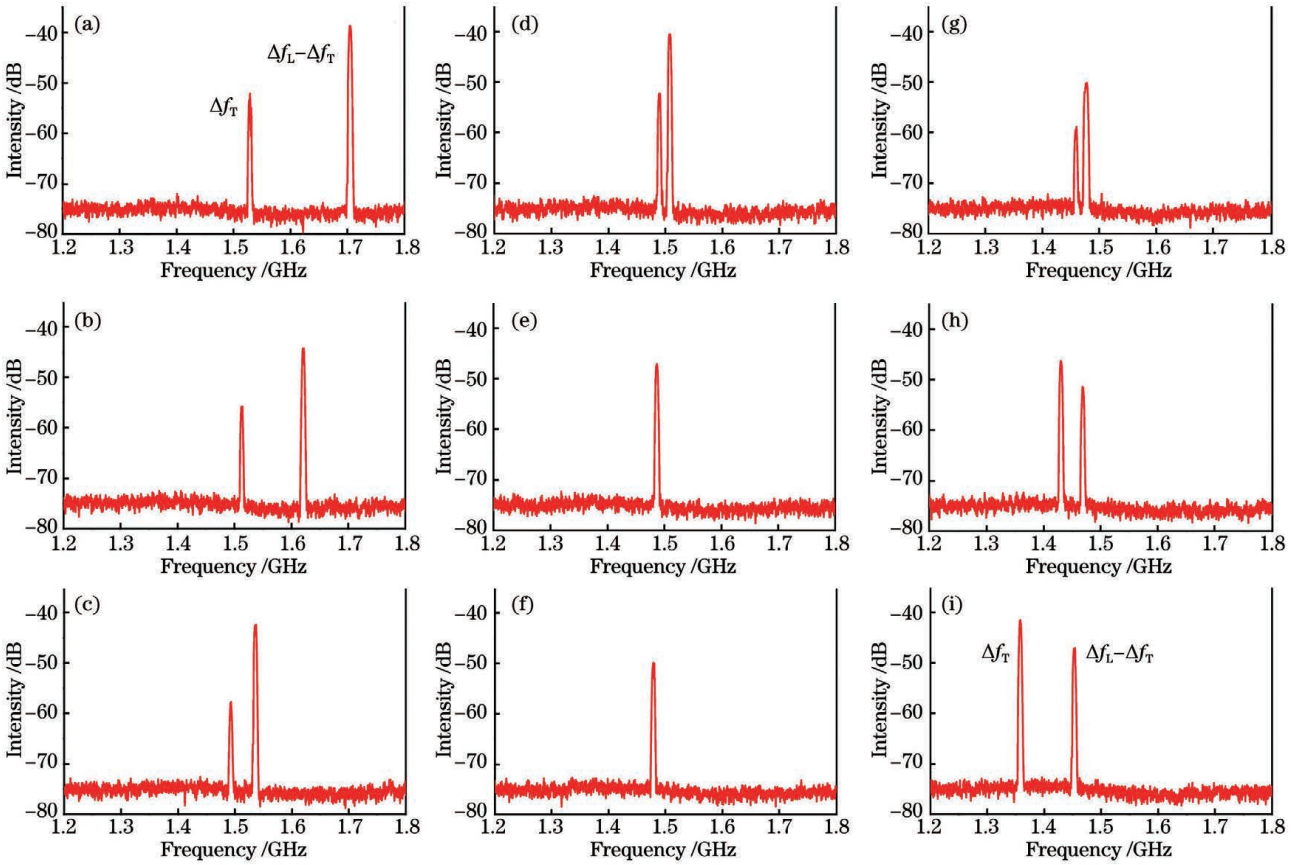

图 5 不同腔长时 1.5 GHz 附近输出激光的频谱图。(a) L=47.25 mm;(b) L=48.25 mm;(c) L=49.85 mm;(d) L=50.35 mm;(e) L=50.65 mm;(f) L=50.85 mm;(g) L=51.25 mm;(h) L=52.25 mm;(j) L=54.25 mm

Fig. 5 Frequency spectra of output laser beams in the vicinity of 1.5 GHz at different cavity lengths. (a) L=47.25 mm; (b) L=48.25 mm; (c) L=49.85 mm; (d) L=50.35 mm; (e) L=50.65 mm; (f) L=50.85 mm; (g) L=51.25 mm; (h) L=52.25 mm; (j) L=54.25 mm

族(简并发生时)的横模在简并位置处发生简并,谐振输出。此外,利用激光频谱的变化,实现了对简并范围的更精确测量,本实验中的简并范围约为 0.20 mm。相较于利用泵浦阈值或输出功率的变化来确定的简并范围,本文提出的利用频谱变化来确定的简并范围更准确。实际应用中,若要利用横模频率简并产生结构光,简并范围精确测量是一个重要的前提条件。本研究结果对横模频率简并的实际应用具有一定的参考价值。

参 考 文 献

[1] Han X, Chen X L, Xiong W, et al. Vaccum optical tweezers system and its research progress in precision measurement[J]. Chinese Journal of Lasers, 2021, 48(4): 0401011.
韩翔, 陈鑫麟, 熊威, 等. 真空光镊系统及其在精密测量中的研究进展[J]. 中国激光, 2021, 48(4): 0401011.

[2] Jesacher A, Fürhapter S, Bernet S, et al. Spiral interferogram analysis[J]. Journal of the Optical Society of America A, 2006, 23(6): 1400-1409.

[3] Fürhapter S, Jesacher A, Bernet S, et al. Spiral phase contrast imaging in microscopy[J]. Optics Express, 2005, 13(3): 689-694.

[4] Tamm C. Frequency locking of two transverse optical modes of a laser[J]. Physical Review A, 1988, 38(11): 5960-5963.

[5] Shen Y J, Wan Z S, Fu X, et al. Observation of spectral modulation coupled with broadband transverse-mode-locking in an Yb∶CALGO frequency-degenerate cavity[J]. Chinese Optics Letters, 2019, 17(3): 031404.

[6] Gorbunkov M V, Kostryukov P V, Tunkin V G. Sharp focusing of superpositions of Hermite-Gaussian modes locked in fractionally degenerate cavity[J]. Laser Physics, 2019, 29(11): 115003.

[7] Chen C H, Wei M D, Hsieh W F. Beam-propagation-dominant instability in an axially pumped solid-state laser near degenerate resonator configurations[J]. Journal of the Optical Society of

America B, 2001, 18(8): 1076-1083.

[8] Lu T H, Chen Y F, Huang K F. Spatial morphology of macroscopic superposition of three-dimensional coherent laser waves in degenerate cavities[J]. Physical Review A, 2008, 77: 013828.

[9] Cheng Z D, Liu Z D, Luo X W, et al. Degenerate cavity supporting more than 31 Laguerre-Gaussian modes[J]. Optics Letters, 2017, 42(10): 2042-2045.

[10] Zhang Q, Ozygus B, Weber H. Degeneration effects in laser cavities[J]. The European Physical Journal Applied Physics, 1999, 6: 293-298.

[11] Bezotosnyi V V, Cheshev E A, Gorbunkov M V, et al. Manifestation of active medium astigmatism at transverse mode locking in a diode end-pumped stable resonator laser[J]. Applied Optics, 2008, 47(20): 3651-3657.

[12] Bezotosnyi V V, Cheshev E A, Gorbunkov M V, et al. Behavior of threshold pump power of diode end-pumped solid-state lasers in critical cavity configurations[J]. Laser Physics Letters, 2015, 12(2): 025001.

[13] Liu K, Li Z, Guo H, et al. Generation of high-order Hermite-Gaussian beams using a spatial light modulator[J]. Chinese Journal of Lasers, 2020, 47(9): 0905004.
刘奎, 李治, 郭辉, 等. 使用空间光调制器产生高阶厄米高斯光束[J]. 中国激光, 2020, 47(9): 0905004.

[14] Li P, Zhang S L, Wang S, et al. High efficiency vortex beam generation by optimization of defect-spot mirror[J]. Chinese Journal of Lasers, 2020, 47(5): 0501005.
李平, 张澍霖, 汪莎, 等. 通过优化损耗点镜产生高效率的涡旋光束[J]. 中国激光, 2020, 47(5): 0501005.

[15] Liu Q, Pan J, Wan Z S, et al. Generation methods for complex vortex structured light field[J]. Chinese Journal of Lasers, 2020, 47(5): 0500006.
柳强, 潘婧, 万震松, 等. 复杂涡旋结构光场的产生方法[J]. 中国激光, 2020, 47(5): 0500006.

[16] Arnaud J A. Degenerate optical cavities[J]. Applied Optics, 1969, 8(1): 189-195.

[17] Francia D G T. Proceedings of the symposium on optical masers[M]. Brooklyn: Polytechnic Press, 1963: 157.

[18] Tung J C, Tuan P H, Liang H C, et al. Fractal frequency spectrum in laser resonators and three-dimensional geometric topology of optical coherent waves[J]. Physical Review A, 2016, 94: 023811.

Frequency degeneracy of transverse modes in Nd∶YVO_4 lasers

Lin Da[1,2], Wang Jing[1,2], Li Bingxuan[1], Liao Wenbin[1], Lin Zhanglang[1], Tang Kaifei[1,3], Li Ke[1,2], Zhang Ge[1*]

[1] *Key Laboratory of Optoelectronic Materials Chemistry and Physics, Fujian Institute of Research on the Structure of Matter, Chinese Academy of Sciences, Fuzhou, Fujian* 350002, *China*;

[2] *University of Chinese Academy of Sciences, Beijing* 100049, *China*;

[3] *College of Chemistry, Fuzhou University, Fuzhou, Fujian* 350108, *China*

Abstract

Objective Structured light has been exploited in several fields in the past two decades, such as optical tweezers, spiral interferometers, and phase-contrast microscopes. The generation of structured light is generally achieved by utilizing optical elements such as spatial light modulators or spiral phase plates. Because of the limit on output power when utilizing these optical elements to generate structured light, a direct generation of structured light is proposed in the laser cavity. Intracavity generation of structured light could be achieved based on the theory of transverse mode degeneracy. The degenerate range (or lock range), which means a special short range of cavity length, is an important condition for exploiting transverse mode degeneracy to generate structured light. When the cavity length is adjusted to the degenerate range, the degeneracy condition is met. When the cavity meets the degeneracy condition, resonant frequencies of specific transverse modes become equal. In this situation, these specific modes will coherently superpose each other and generate a light field that may exhibit spatial structure. Therefore, the accurate degenerate range plays an important role in utilizing this method to generate structured light. Thus, to the approach of measuring the accurate degenerate range becomes a significant issue, which is what we mainly consider in this

research.

Methods The degenerate range is determined by the variation of output power or threshold of pump power in some articles. However, the widths of the degenerate range determined using these methods are somewhat approximate; their precision could be improved using other measurement methods. To more accurately measure the degenerate range, we try to exploit the frequency spectra of laser beams to characterize the degenerate range in this paper. As the cavity length is tuned slowly in the experiment, the frequency spectra of laser beams are detected in detail. Two peaks in the spectra that particularly considered in this study to show an obvious process of merging as the confocal resonator approaches the degenerate position. In this paper, the range of cavity length in which the two peaks become superposed is defined as the degenerate range. This type of measurement method is more accurate than the methods that utilize the variation of output power or threshold of pump power to determine the degenerate range because it directly monitors the variation of frequency spectra. We use the frequency spectra measured in experiment to analyze the change of dynamic behavior of transverse modes with different orders.

Results and Discussions The frequency data measured in the experiment are shown in Fig. 3. As the cavity length changes, each of these frequencies (Δf_{L}, $2\Delta f_{\mathrm{T}}$, $\Delta f_{\mathrm{L}}-\Delta f_{\mathrm{T}}$, Δf_{T}, and $\Delta f_{\mathrm{L}}-2\Delta f_{\mathrm{T}}$) show a variation tendency consistent with the theoretical variation tendency. Variations of these detected frequencies indicate the change of dynamic behavior of transverse modes with different orders. By analyzing these frequency spectra, we find that even though competition between modes exists, transverse modes that belong to different degenerate families are not suppressed when degeneracy occurs. The frequency difference of modes with the same order is clearly detected in the vicinity of the degeneration point, and it is not observed away from the degeneration point. From the beam patterns (Fig. 4), we can observe that higher-order transverse modes are generated when the confocal resonator is tuned in the vicinity of the degeneration point. This phenomenon implies that as the resonant frequency of the high-order mode becomes equal to that of the low-order mode, the high-order mode becomes easier to generate in the cavity. The detailed frequency spectra are presented in Fig. 5, using which we determine the degenerate range. As the confocal resonator is tuned to the degeneration point, the two peaks ($\Delta f_{\mathrm{L}}-\Delta f_{\mathrm{T}}$ and Δf_{T}) become closer to each other and finally superpose. The state in which these two peaks are superposed sustains for a short range of cavity lengths. Accordingly, we could obtain the width of the degenerate range, which is approximately 0.20 mm in this experiment. The degenerate range defined in this way ought to be more accurate because it is directly determined from frequency spectra.

Conclusions In this paper, the phenomenon of transverse mode degeneracy is researched based on the variation of frequency spectra, and a more accurate method for measuring the degenerate range (or lock range) is proposed. As the cavity length varies in the experiment, frequency spectra of laser beams are recorded in detail. The variation of dynamic behavior of transverse modes before and after the degeneracy is analyzed based on the frequency spectra. When the cavity satisfies the degeneracy condition, the two degenerate families of transverse modes (in 1/2 degeneracy) coexist in the cavity, neither of them is suppressed because of the competition between them. Meanwhile, the beam patterns measured in the experiment show that higher-order transverse modes are generated when degeneracy occurs. As the resonant frequency of the high-order transverse mode becomes degenerate with that of the low-order mode, the high-order mode becomes easier to generate, thus resonating with the low-order mode in the cavity. We achieve a more accurate measurement of the degenerate range with the frequency spectra measured in the experiment. The degenerate range is approximately 0.20 mm in this experiment. It exhibits a higher precision and is more accurate than the degenerate range determined using other methods. The results of this paper may provide some reference value for the application of transverse mode degeneracy.

Key words lasers; transverse modes; frequency spectra; degeneracy; degenerate range

OCIS codes 140.3070; 140.3480; 140.4050